ACS SyntheticBiology

pubs.acs.org/synthbio

Research Article

Design, Evolution, and Characterization of a Xylose Biosensor in *Escherichia coli* Using the XylR/*xylO* System with an Expanded Operating Range

Rui-Qi Tang, James M. Wagner, Hal S. Alper,* Xin-Qing Zhao,* and Feng-Wu Bai

Cite This: *ACS Synth. Biol.* 2020, 9, 2714–2722

Read Online

ACCESS | Metrics & More | Article Recommendations | Supporting Information

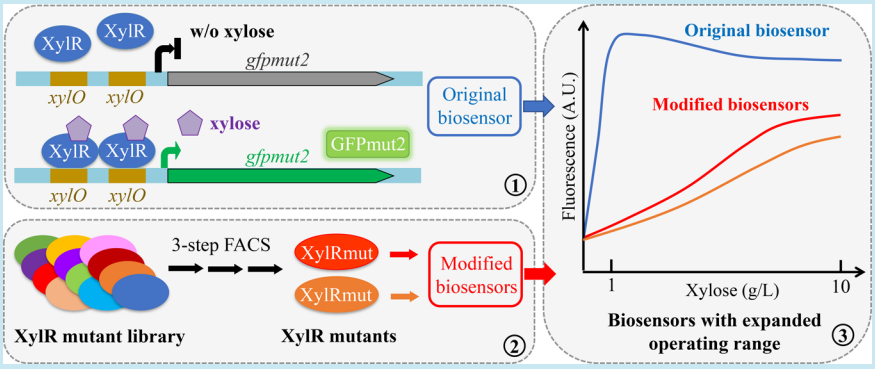

ABSTRACT: Genetically encoded biosensors are extensively utilized in synthetic biology and metabolic engineering. However, reported xylose biosensors are far too sensitive with a limited operating range to be useful for most sensing applications. In this study, we describe directed evolution of *Escherichia coli* XylR, and construction of biosensors based on XylR and the corresponding operator *xylO*. The operating range of biosensors containing the mutant XylR was increased by nearly 10-fold comparing with the control. Two individual amino acid mutations (either L73P or N220T) in XylR were sufficient to extend the linear response range to upward of 10 g/L xylose. The evolved biosensors described here are well suited for developing whole-cell biosensors for detecting varying xylose concentrations across an expanded range. As an alternative use of this system, we also demonstrate the utility of XylR and *xylO* as a xylose inducible system to enable graded gene expression through testing with *β*-galactosidase gene and the lycopene synthetic pathway. This evolution strategy identified a less-sensitive biosensor for real applications, thus providing new insights into strategies for expanding operating ranges of other biosensors for synthetic biology applications.

KEYWORDS: *xylose biosensor, inducible system, Escherichia coli, XylR, directed evolution, expanded operating range*

Synthetic control elements that regulate the expression and conditional response of genes are key research targets for metabolic engineering to dynamically control product yield and minimize cell burden,[1,2] as well as for biosensing applications[3] to detect analyte levels. Among the choices of regulatory elements, the use of responsive transcription factors and corresponding promoters/operators is a promising approach, and has been successful in a wide variety of strain development applications.[4,5] Likewise, the capacity for regulatory elements to sense small molecules is useful in common induction systems.[6] However, many initially constructed biosensors do not meet the demand of real applications, and thus further improvements such as breadth of detectable analytes or usable dynamic range may be required to enable specific applications. Directed evolution is commonly used to alter the performance of transcriptional factor-based biosensors.[7,8] By using fluorescence-activated cell sorting (FACS) and other high-throughput screening methods, targets that reach the requirements would be obtained in a relatively short time and with less labor.[3,9]

Among the choices for endogenous biosensors, alternative substrate utilization pathways afford an interesting starting point for biosensor development. Two well-studied examples include the native *Escherichia coli* arabinose and xylose regulators encoded by *araC* and *xylR*, respectively.[6,10] Although the AraC/P_{BAD} regulator/promoter system has been widely utilized on account of its tight regulation and strong response in the induced state,[6] limited focus has been

Received: April 23, 2020
Published: September 4, 2020

https://dx.doi.org/10.1021/acssynbio.0c00225
ACS Synth. Biol. 2020, 9, 2714–2722

placed on studying and applying the *E. coli* XylR and its related operator *xylO* as a biosensing system for inducible gene expression.[11−13] Mechanistically, *E. coli* XylR functions as a transcriptional activator and regulates the expression of the xylose utilization genes (*xylAB*) and transporter genes (*xylFGH*) in response to xylose.[14] Specifically, in the absence of xylose, XylR is unable to bind to *xylO*, and expression of the downstream genes is repressed, while in the presence of xylose, XylR binds to xylose and two XylR proteins form a homodimer that activates gene expression (Figure 1) in concert with

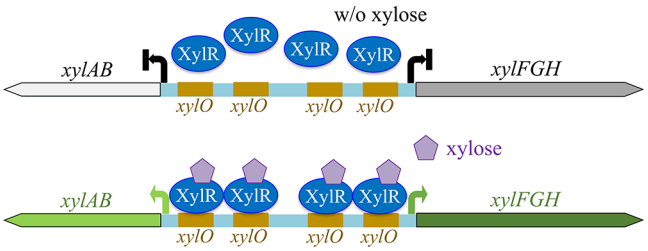

Figure 1. Schematic of XylR-regulated gene expression. In the absence of xylose, XylR cannot bind to xylO and expression of xylAB and xylFGH is repressed. In the presence of xylose, XylR binds to xylose and then binds to xylO, initiating the expression of xylAB and xylFGH.

activated CRP (cAMP receptor protein).[14] In the previous studies, the *E. coli xylF* promoter (*PxylF*)[11] and *xylA* promoter (*PxylA*)[12] have been demonstrated as being xylose-inducible, indicating the feasibility of constructing a functional whole-cell xylose biosensor based on *E. coli* XylR and the operator *xylO* that is present in *PxylF* and *PxylA*.[14]

Xylose can be released by simple hydrolysis of lignocellulosic biomass, and is the second most abundant monosaccharide after glucose. Due to the fact that xylose can be converted to biofuels and various high value-added chemicals by diverse microorganisms, it is always of great interest to develop xylose-utilizing microbial cell factories.[15−17] In the previous reports, by using a xylose-responsive system, xylose biosensors were constructed in budding yeast *Saccharomyces cerevisiae* using *xylR* genes from various prokaryotic microbes such as *Tetragenococcus halophile*,[18] *Lactobacillus pentosus*,[18] *Clostridium difficile*,[18] *Staphylococcus xylosus*,[19] *Bacillus licheniformis*,[19] *B. subtilis*,[19] and *Caulobacter crescentus*.[20] The operating range varies in these cases from 0.001−0.1 g/L xylose[20] to 4−100 g/L xylose.[18] However, these XylRs are transcriptional repressors, different from the *E. coli* XylR which is a transcriptional activator.[14] In a recent work, *E. coli* XylR and its operator *xylO* were utilized in *Yarrowia lipolytica* and exhibited dose-dependent gene expression in a xylose range from 0 to 3 g/L.[13] Nevertheless, to date, no study has been performed on evolution of *E. coli* XylR and development of the XylR/*xylO* system as a biosensor in *E. coli*. One of the most widely used inducible systems in *E. coli* is the AraC/P_{BAD}, which could be used as a reference since it possesses the most similar regulatory mechanism with the XylR/*xylO* system. The AraC/P_{BAD} system regulates graded gene expression in *E. coli* also at very low concentration levels (less than 1 g/L).[21] This type of response dynamics is not optimal when the whole-cell *E. coli* xylose biosensor is used to detect xylose at much higher concentration range in lignocellulosic hydrolysate or to screen xylose-utilizing strains. In this regard, it is of great importance to design and develop a xylose biosensor that does not exist in nature with a suitable operating range for applications in strain development.[22]

Here we report on the directed evolution of XylR and development of xylose biosensors based on the resultant mutants and the operator *xylO*. Our current report demonstrates the first broadening of the operational range of the xylose-responsive biosensor and developing of novel biosensors for this important sugar. Furthermore, we extended the utility of this system to enable a graded gene expression through testing with an alternative enzyme (*β*-galactosidase) and a biosynthetic pathway (lycopene biosynthetic genes), which demonstrate that the XylR/*xylO* system can also be used to regulate gene expression using xylose as an inexpensive inducer.

RESULTS AND DISCUSSION

Establishing a System for Xylose Biosensor Functional Expression. To enable *E. coli* to serve as a whole-cell biosensor for xylose, it is necessary to remove the catabolic enzymes that would otherwise degrade this inducer. To do so, we deleted the *xylA* and *xylB* genes, which were previously reported to abolish growth on xylose, but not transport of xylose.[14] Next, we also deleted the endogenous *xylR* gene to better study the function of the *xylR*-based xylose biosensor, thus establishing the strain NEB10*β*-ΔxylR-ΔxylAB. Specifically, we found that this strain indeed did not consume xylose over the course of 24 h incubation. Xylose was not utilized even when *xylR* was overexpressed in this strain (Figure S1).

With this catabolism-null background strain in place, we next turned to creating a construct using the wild-type *xylR* regulator (*xylR-WT*) to induce the expression of the green fluorescence protein mutant (GFPmut2).[22] To do so, we cloned the entire intergenic region between *xylA* and *xylF* to serve as the inducible promoter system based on the prior evidence.[11,12,14] The map of the constructed plasmid is shown in Figure S2. Next, this biosensor was transformed into the above-described strain and tested for function across varying xylose concentrations. As expected, a graded response in fluorescence to different xylose concentrations was observed only for concentrations less than 1 g/L xylose (Figure 2) with full saturation seen at concentrations above this level. This system thus served as the starting point for engineering efforts to extend the operated range *via* a directed evolution strategy.

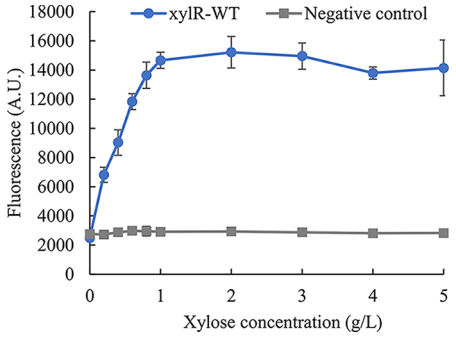

Figure 2. Fluorescence response of biosensor based on wild-type xylR (xylR-WT) to xylose. Strain NEB10*β*-ΔxylR-ΔxylAB-xylR-WT-GFPmut2 was grown in the presence of different xylose concentrations. Strains were incubated at 30 °C with 1000 rpm shaking for 5 h. Results represent the mean ± SE of triplicates.

https://dx.doi.org/10.1021/acssynbio.0c00225
ACS Synth. Biol. 2020, 9, 2714−2722

Expanding the Operating Range of XylR-Based Biosensors through Directed Evolution. To reduce the overall sensitivity of XylR to xylose and thus expand the operating range of the biosensor, we utilized a directed evolution strategy aided by error-prone polymerase chain reaction (ep-PCR). To enable random mutations in an unbiased manner across the entire protein including all functional elements of XylR (especially the DNA binding, xylose binding or dimerization activity), the forward and reverse primers (xylR-F/-R, Table S3) were designed to amplify the entire open reading frame from the start codon to the stop codon of *xylR*. As the goal here is to take an already functioning sensor and expand its range, it was not sufficient to simply sort for high fluorescence at higher concentrations of xylose. As a result, it is necessary to perform a series of iterative FACS-based sorting using alternating conditions and gates. Specifically, all of the transformants were subjected to a three-step sorting process, in which (i) all cells exhibiting fluorescence in high xylose concentration (10 g/L) were collected, followed by (ii) the bottom 15% of fluorescing cells under the induction condition of lower xylose concentration (1 g/L) and (iii) the middle 15% of fluorescing cells under moderate xylose concentration (5 g/L) were collected. After this sorting, cells were collected and plated onto LB agar containing 10 g/L xylose as a secondary screen under blue light to select for green fluorescent colonies. Using this strategy, 10^6−10^7 sized libraries were sorted in a first pass analysis followed by individual performance analysis of a few hundred candidates on a flow cytometer, and eventually obtained our final two selected mutants *xylRmut17* and *xylRmut36* (encoding $XylR^{N220T}$ and $XylR^{L73P,S370A}$, which is described in the following section) that exhibited promising performance.

To better evaluate the performance of these mutants, we evaluated fluorescence response of the NEB10*β*-ΔxylR-ΔxylAB strain harboring the xylRmut17-GFPmut2, xylR-mut36-GFPmut2, and xylR-WT-GFPmut2 constructs in the presence of 0 to 10 g/L xylose with 1 g/L as an interval (Figure 3 and Figure S3). When evaluating the response curves, the lower slopes associated with mutant biosensors *xylRmut17* and *xylRmut36* (0.64 and 0.53, respectively) compared to the wild-type biosensor *xylR-WT* (1.01) indicate the achieved reduced sensitivity of the mutant biosensors (Figure S3). Consistently, in contrast to the wild-type *xylR* based biosensor, these mutants showed the desired expanded operating range with respect to xylose (Figure 3). Besides, the similar expanded operating range was also observed in *xylRmut17* regulated expression of a red fluorescence protein encoding gene *mKate2* (Figure S4). The xylose biosensors containing the *xylR* mutants exhibited linear response to xylose concentration up to 10 g/L, which places these sensors in the range for detecting xylose from more bioprocessing meaningful concentrations. It is worth mentioning that the increase of fluorescence in the presence of xylose was the result of a shift in expression across the whole population compared to that under the uninduced condition, indicating that the biosensor exhibited no population heterogeneity under the conditions used in this study (Figure S5).

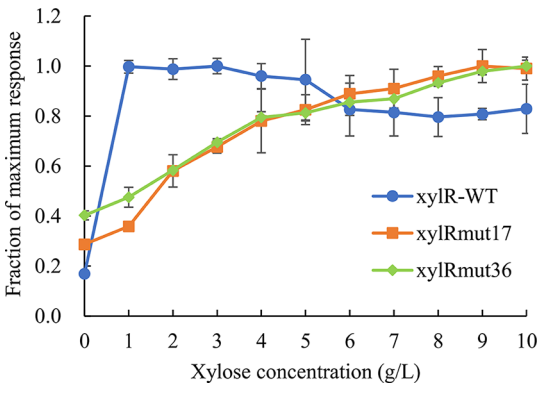

Figure 3. Comparative response of mutant biosensors. The fraction of maximum response for biosensors using wild-type xylR (xylR-WT), xylRmut17, and xylRmut36 across a range of different xylose concentration was evaluated after 5-h induction at 30 °C, with 1000 rpm shaking. Results represent the mean ± SE of duplicates.

To confirm the genotype of the mutants with reduced XylR activity as well as the underlying causative mutations, *xylRmut17*, and *xylRmut36* were sequenced. From this, we identified that *xylRmut17* contained one mutation (A659C) that results in a coding mutation for $XylR^{N220T}$. Two mutations were identified in *xylRmut36* (T218C and T1108G) that are also both coding mutations resulting $XylR^{L73P,S370A}$. On the basis of the crystal structure of XylR,[10] mutation sites N220T and L73P are close to the xylose binding site, whereas mutation S370A is located more distally.

To understand the functional consequence of these mutations, we evaluated each of the mutations separately as well as in combination of all three identified mutations to see if there were potential synergies. These mutations were all evaluated in the same NEB10*β*-ΔxylR-ΔxylAB background using GFP-based fluorescence as the read-out (Figure 4). Two

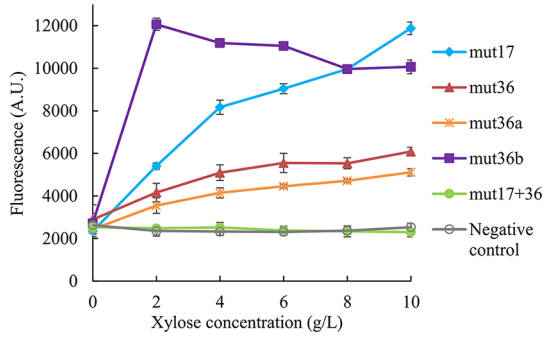

Figure 4. Causative mutation analysis of XylR mutants. Fluorescence response of strains with biosensors containing XylRmut17, XylRmut36, XylRmut36a (only containing the mutation site of L73P), XylRmut36b (only containing the mutation site of S370A), and XylRmut17+36 (all three identified mutations combined). Results represent the mean ± SE of triplicates.

major trends are observable from this data. First, it is quite obvious that L73P was the causative mutation in XylRmut36 since the single mutation of $XylR^{L73P}$ (XylRmut36a) behaved similarly to XylRmut36, whereas the S370A mutation (XylRmut36b) reverted the function to a pattern similar to the wild-type XylR (Figure 2). Second, it was rather surprising to see that the combination of all three mutations (XylRmut17+36 that contains L73P, N220T, and S370A) was essentially inactive and exhibited no response to xylose. To further evaluate this combination and determine the underlying cause, mutants $XylR^{L73P,N220T}$ and $XylR^{N220T,S370A}$ were constructed and tested in the presence of 10 g/L xylose (Figure S6). We observed here that the sensor failed to

https://dx.doi.org/10.1021/acssynbio.0c00225
ACS Synth. Biol. 2020, 9, 2714−2722

function with the combination of N220T and L73P, demonstrating that the two mutations close to xylose binding site completely inactivated the xylose binding activity of XylR.

Since the overall operating range for this sensor was improved, it is important to be sure that this does not result in an increase of promiscuity. To do so, we evaluated the response of strains carrying biosensors with *xylR-WT*, *xylRmut17*, and *xylRmut36* to other monosaccharides (glucose, arabinose, and galactose) (Figure 5). We observed a nearly

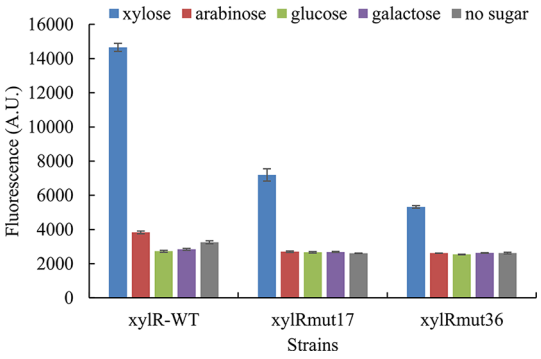

Figure 5. Fluorescence response of *E. coli* strains with biosensors containing xylR-WT, xylRmut17, and xylRmut36 to 10 g/L of various sugars, including xylose, glucose, arabinose, and galactose. Fluorescence in LB with no sugar was used as negative control. Strains were incubated at 30 °C with 1000 rpm shaking for 5 h. Results represent the mean ± SE of triplicates.

exclusive recognition of xylose across the board with high specificity for these two new mutant versions. In fact, the slight response to arabinose seen in the wild-type version was not seen with these mutants, suggesting that promiscuity was reduced in this study.

Collectively, these results demonstrate a successful engineering effort to reduce the sensitivity of a biosensor in an effort to expand the operating range. In some respects, this strategy searched for a "worse" biosensor evolutionarily, thus providing new insights in biosensor evolution. In this regard, it should be noted that the FACS strategy used here can also be generally applied to other catabolic sensors (such as the arabinose biosensor) that exhibit a linear response to arabinose in a very low range of concentrations (less than 0.1 g/L, Figure S7). Additionally, *E. coli* cells with the evolved biosensor could act as a whole-cell biosensor in a manner that is more efficient than HPLC and enzymatic methods and amenable to high-throughput screening.

Further Characterization of Biosensor Dynamic Response. To further characterize the graded response of these mutant biosensors, we detected real-time response to xylose-based regulation *via* fluorescence and biomass accumulation using a BioLector Pro system (m2p-labs, Germany). GFP expression of the cells was normalized to biomass and fluorescence fold changes under different xylose concentrations were compared to the absence of xylose (Figure 6). In general, these whole population responses had trends that are consistent with the single cell data (Figure 3). Specifically, the two mutants show a more graded response with respect to xylose concentration (as can be seen by a separation of the curves) compared with that of the wild-type that showed little variation across concentrations (comparing Figures 6B, C with 6A). Likewise, the maximum fold change of fluorescence for *xylRmut17* (~5.9, Figure 6B) and *xylRmut36* (~4.8, Figure

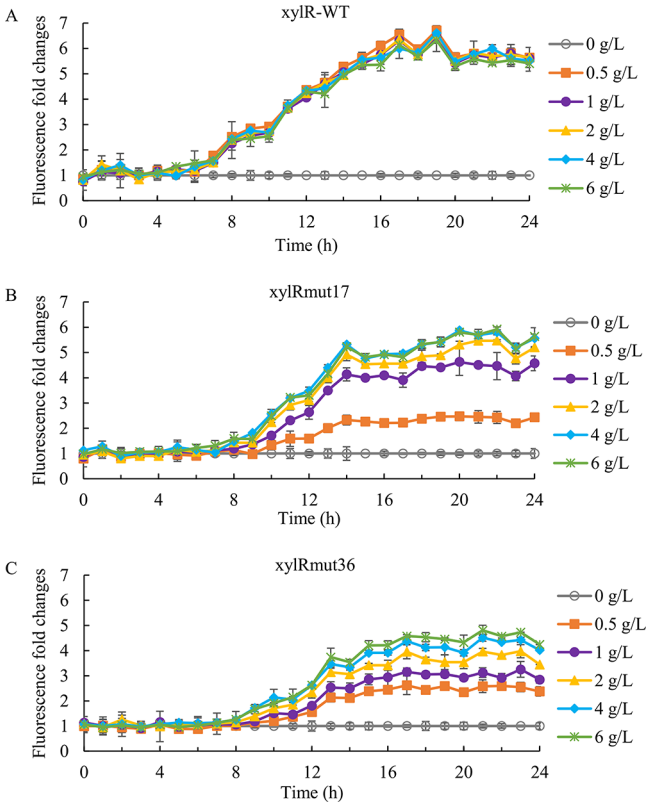

Figure 6. Bulk culture-based analysis of biosensors using BioLector PRO system. The fold changes of fluorescence in strains carrying xylose biosensor with xylR-WT (A), xylRmut17 (B), and xylRmut36 (C) are continuously monitored across 24 h in LB with 0, 0.5, 1, 2, 4, and 6 g/L xylose under 30 °C. Results represent the mean ± SE of duplicates.

6C) were both lower than that of strain harboring the *xylR-WT* construct (~6.6, Figure 6A). The only deviation between the experiments was seen for *xylRmut17* that showed little difference using 4 and 6 g/L xylose in 24-h dynamic assay, whereas this was not the case in test tube-based culturing followed by FACS. Nevertheless, these whole population responses are consistent with the results seen in the single cell fluorescence values, thus demonstrating reliable induction.

As a final characterization of the biosensor response, we utilized quantitative PCR using the *xylRmut17* as an example to determine that the response of these elements was indeed at the transcriptional level. As shown in Figure S8, there was indeed a strong linear relationship between GFP fluorescence and transcript (R^2 = 0.977), indicating the transcriptional activator response of this element.

Expansion of the Xylose Biosensor for an Alternative Protein-Encoding Gene. To validate that the mutant biosensor can regulate gene expression more generally, we tested an alternative reporter protein, *β*-galactosidase, in the presence of various xylose concentrations. Xylose concentrations used here were determined based on the BioLector results (Figure 6), where the fluorescence showed little difference when tested in the presence of 4 g/L and 6 g/L xylose. After 15-h induction in 0, 0.5, 1, 2, 3, and 4 g/L xylose, cells of NEB10*β*-ΔxylR-ΔxylAB-xylR-WT-lacZ and NEB10*β*-ΔxylR-ΔxylAB-xylRmut17-lacZ were evaluated for *β*-galactosidase activity (Figure 7A). In contrast to the conditions of GFP, the maximum response showed no significant difference

https://dx.doi.org/10.1021/acssynbio.0c00225
ACS Synth. Biol. 2020, 9, 2714−2722

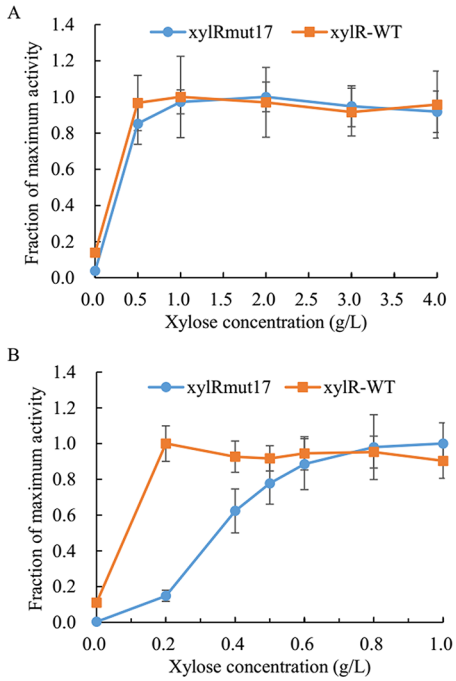

Figure 7. Evaluation of an alternative reporter protein. Fraction of maximum β-galactosidase activity of strains NEB10β-ΔxylR-ΔxylAB-xylR-WT-lacZ and NEB10β-ΔxylR-ΔxylAB-xylRmut17-lacZ was tested after 15-h incubation at 30 °C. Xylose concentrations used were 0, 0.5, 1, 2, 3, and 4 g/L (A) and 0, 0.2, 0.4, 0.5, 0.6, 0.8, and 1 g/L (B). Results represent the mean ± SE of triplicates.

between biosensors with *xylR-WT* and *xylRmut17* when xylose concentration was changed from 1 g/L to 4 g/L. Therefore, β-galactosidase activity in the presence of 0, 0.2, 0.4, 0.5, 0.6, 0.8, and 1 g/L xylose was measured, it was seen that total maximum β-galactosidase plateaued rather quickly, but differences in the operating range were still observed for the *xylRmut17 vs xylR-WT* across a range of xylose concentrations, and the mutant had more of a dynamic response than that of the wild-type (Figure 7B). We deduced three possible reasons for the reduced operating range of *lacZ* induction compared to the GFP induction: (i) different reporters, the *lacZ* gene is much larger than GFP gene (3075 bp *vs* 747 bp), and also the fluorescence protein and enzyme protein could exhibit different expression and degradation pattern; (ii) different incubation time, to provide reference to further pathway regulation with this system, we increased the induction time of β-galactosidase to 15 h, whereas we used 5 h for the GFP system; and (iii) different detecting methods, the fluorescence was detected in a single cell, while the enzyme activity was examined for the whole cell population.

Regulating a Downstream Pathway *via* the Mutant Xylose Biosensor-Promoter System. As a final demonstration of the utility of the mutant biosensor beyond its application as a whole cell-biosensor for xylose concentration in a culture, we evaluate the utility of this promoter system to regulate an entire pathway. In this case, we chose to evaluate lycopene, a potent antioxidant that can be produced by overexpressing three heterologous genes encoding pyrophosphate synthase (*crtE*), phytoene synthase (*crtB*) and phytoene desaturase (*crtI*).[24,25] In this example, we sought to evaluate the utility of this biosensor by also testing in a strain without *xylAB* deletion to determine the performance of the induction system when xylose could be utilized by the strain.

Through evaluating response across a range of xylose induction concentrations, lycopene production in strains NEB10β-ΔxylR-xylRmut17-crtEBI and NEB10β-ΔxylR-ΔxylAB-xylRmut17-crtEBI reached the maximum levels at 0.6 g/L and 0.4 g/L xylose, respectively (Figure 8A). However,

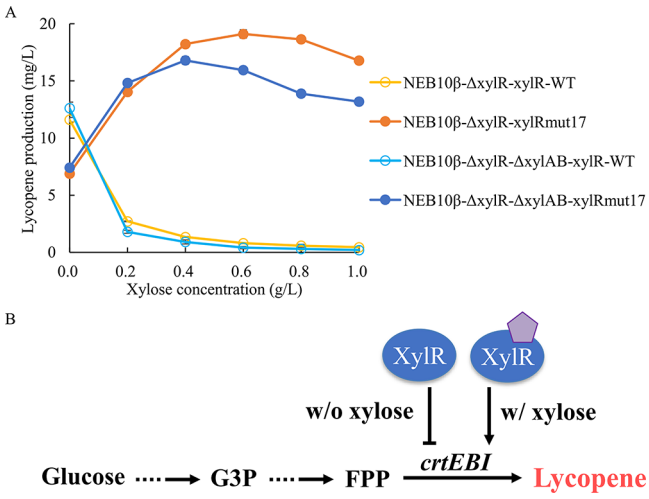

Figure 8. Lycopene production under the control of XylR-WT and XylRmut17 in strains NEB10β-ΔxylR and NEB10β-ΔxylR-ΔxylAB (A), and regulation of lycopene production (B). Lycopene production in strains NEB10β-ΔxylR-xylR-WT-crtEBI, NEB10β-ΔxylR-xylRmut17-crtEBI, NEB10β-ΔxylR-ΔxylAB-xylR-WT-crtEBI, and NEB10β-ΔxylR-ΔxylAB-xylRmut17-crtEBI in the presence of 0, 0.2, 0.4, 0.5, 0.6, 0.8, and 1 g/L xylose. Cells were cultivated at 30 °C for 15 h, and 1 mL cell culture was prepared for lycopene extraction. Results represent the mean ± SE of triplicates.

significantly lower lycopene production was observed in strains with *xylR-WT* (Figure 8A), indicating the advantage of mutant *xylR* in the regulation of lycopene production. Despite the lower operating range compared to the results of GFP, the mutant *xylR* still showed better performance as a gene expression regulator than *xylR-WT*, and can be used to tune the optimal expression level of pathway enzymes. Moreover, we observed a reduction of cell density at higher xylose concentrations here in NEB10β-ΔxylR-ΔxylAB strain background which cannot utilize xylose (Figure S9). This result is consistent with the IPTG- or arabinose-induction patterns in previous work,[26] indicating the cell burden caused by overexpressing lycopene synthetic pathway.[27] Across these two strain backgrounds, it was noted that production of lycopene was higher in NEB10β-ΔxylR compared with the NEB10β-ΔxylR-ΔxylAB, potentially due to the conversion of xylose as a carbon source and continued degradation of the inducer signal which subsequently reduces metabolic burden of the cells (Figure 8A and B). In summary, graded regulation of gene expression by the mutant biosensor was demonstrated in both strain backgrounds. Limitations of the lycopene pathway notwithstanding, we still found higher lycopene production regulated by the mutant XylR comparing with that regulated by the wild-type XylR. The results demonstrated that the xylose-induced gene expression system could be applied in inducible control of gene expression, a useful technique for metabolic engineering applications.[28]

In summary, we have demonstrated that a transcriptional activator from alternative sugar catabolism can be evolved to obtain a suitable operating range that better matches

https://dx.doi.org/10.1021/acssynbio.0c00225
ACS Synth. Biol. 2020, 9, 2714−2722

concentrations found in culture media. In particular, the typical binary response curves were extended through this decreased specificity for the analyte. In doing so, we established a generalizable procedure for FACS to obtain a linear response range to upward of 10 g/L xylose, thus enabling future applications as whole-cell biosensors. Furthermore, the evaluation of this system with the alternative models of the *β*-galactosidase gene *lacZ* and the lycopene biosynthetic pathway gene cluster *crtEBI* demonstrated that graded response to xylose was transferrable. The design principle and the XylR/*xylO* system with the XylR mutants developed in this study is well suited for future synthetic biology and metabolic engineering applications.

METHODS

Strains and Plasmids Construction. All the strains and plasmids used in this study were listed in Table S1 and Table S2, respectively. All the primers used in this study were purchased from Integrated DNA Technologies (USA) and listed in Table S3. All the enzymes used in this study were purchased from New England Biolabs (USA), unless otherwise specified.

E. coli strain used in this study is NEB10*β* (New England Biolabs, USA). Luria−Bertani (LB) medium (Teknova, USA) containing 5 g/L yeast extract, 10 g/L tryptone and 10 g/L NaCl was used for *E. coli* strains cultivation. SOC medium which consists of SOB (BD, USA) and 2 g/L glucose was used for transformants recovery. Deletion of genes *xylAB* (adjacent *xylA and xylB*) and *xylR* in NEB10*β* was completed using a *λ*-red system-based method.[29] DNA fragments for *xylAB* and *xylR* deletion were amplified by PCR with Q5 Hot Start High Fidelity DNA Polymerase using primers JMW-0909/-0910 and JMW-0913/-0914, respectively, and the plasmid pKD13 was used as a template. One microgram DNA fragment was added to 50 *μ*L *E. coli* competent cells and the mixture was placed in a 2 mm electroporation cuvette (BioExpress, USA). Electroporation was performed by using Gene Pulser Xcell (Bio-Rad, USA) with the preset program "*E. coli*-2 mm-2.5 kV". Transformants were recovered with 300 *μ*L SOC medium for 2 h and plated on LB agar (20 g/L) containing 25 *μ*L/mL kanamycin (Gold Biotechnology, USA). Single colonies were picked from plates and grown overnight in 3 mL LB with 50 *μ*L/mL kanamycin. Genomic DNAs of cells were extracted using Wizard Genomic DNA Purification Kit (Promega Corporation, USA). Successive deletion of *xylR* and *xylAB* was confirmed by PCR using primers xylR-vKO-F/-R and xylAB-vKO-F/-R. Kanamycin resistance gene was removed according to the method described previously.[29] The resulting strain was named as NEB10*β*-ΔxylR-ΔxylAB. *E. coli* cells were incubated at 30 °C in this study, unless otherwise specified. Xylose concentration in medium was measured by high performance liquid chromatography (HPLC), using Aminex HPX-87H column (Bio Rad, USA) with 0.6 mL/min flow rate, 65 °C column temperature and 50 °C detection temperature of refractive index detector and 5 mM H_2SO_4 as mobile phase.

Plasmid constructs were obtained by Gibson assembly[30] in most cases in this study. An initial xylose biosensor plasmid pXylA-mKate2, which contains *xylR* expression cassette from *E. coli* K-12 strain and mKate2 gene controlled by the intergenic region between *xylA* and *xylF* (referred to as *xylO*) from *E. coli* K-12 strain, was constructed. Red fluorescence protein encoding gene *mKate2* was amplified from pJKR-H-benM (Addgene plasmid # 73925). For better application in the future study, mKate2 gene was replaced by GFPmut2 gene,[23] plasmid backbone was changed to shortened pRS41H (pRS41Hs), resulting plasmid pRS41Hs-xylR-WT-GFPmut2. Plasmid pRS41Hs was constructed by ligation (T4 DNA ligase) of restriction enzyme *Pst*I-digested DNA fragment obtained by linearization of plasmid pRS41H using primers M13-F/*Pst*I-pRS41H-R. Cells were plated on LB agar containing 100 *μ*L/mL ampicillin (Gold Biotechnology, USA) after electroporation. Single colonies were picked and grown overnight in 3 mL LB. Plasmids were extracted by GeneJET Plasmid Miniprep Kit (Thermo Scientific, USA) from the overnight culture and confirmed by *Pst*I digestion. *E. coli* strains carrying plasmid pRS41Hs-xylR-WT-GFPmut2 and empty plasmid pRS41Hs were constructed (NEB10*β*-ΔxylR-ΔxylAB-xylR-WT-GFPmut2 and NEB10*β*-ΔxylR-ΔxylAB-pRS41Hs). Strains carrying pRS41Hs-based plasmid were incubated in LB with 100 *μ*L/mL ampicillin in this study. Unless otherwise specified, LB mentioned in the following text represents LB with 100 *μ*L/mL ampicillin.

In order to compare the arabinose-induced GFP production and xylose-induced GFP production, plasmid with *araC* expression cassette and $araP_{BAD}$-controlled GFPmut2 gene was constructed. First, GFPmut2 gene was amplified from plasmid pRS41Hs-xyR-GFPmut2 and assembled in plasmid pKD46. Then, fragment with *araC*-$araP_{BAD}$-*gfpmut2* was amplified with primers ara-cassette-F/GFP-TAA-R, and assembled in pRS41Hs-xylR-WT-GFPmut2 which was linearized by PCR using primers GFP-TAA-F/*Pst*I-pRS41H-R, replacing the whole cassette of *xylR-xylO-gfpmut2*. The resulting plasmid was named as pRS41Hs-ara-GFPmut2 and the corresponding strain was NEB10*β*-ΔxylR-ΔxylAB-ara-GFPmut2.

For further investigating the performance of the *xylR*-based biosensor, GFPmut2 gene was replaced by *β*-galactosidase (EC: 3.2.1.23) encoding gene *lacZ* and the gene cluster of lycopene synthetic pathway *crtEBI*.[25] Gene *lacZ* was amplified from genomic DNA of *E. coli* MG1655 using primers lacZ-F/-R. Gene cluster *crtEBI*[25] was amplified from plasmid pACYC-yccFS-crtEBI-T7term using primers crtEBI-F/-R. pRS41Hs plasmid backbone was amplified using primers pRS41Hs-backbone-F/-R. The resulting plasmids were named as pRS41Hs-xylR-WT-lacZ and pRS41Hs-xylR-WT-crtEBI, and transformed into strain NEB10*β*-ΔxylR-ΔxylAB, resulting strains NEB10*β*-ΔxylR-ΔxylAB-xylR-WT-lacZ and NEB10*β*-ΔxylR-ΔxylAB-xylR-WT-crtEBI.

Mutant Library Construction and Screening. Error-prone PCR was performed using GeneMorph II Random Mutagenesis Kit (Agilent Biotechnologies, USA) with primers xylR-F/-R and template pRS41Hs-xylR-WT-GFPmut2. Specifically, high target DNA amount (500 ng) and low cycle numbers (20 or 25) were used for generating mutant *xylR* genes to ensure a low mutation rate of one or two amino acid mutations per XylR protein. Mutation rate was confirmed by sequencing. PCR products from 20 cycle number and 25 cycle number reactions were purified by GeneJET Gel Extraction Kit (Thermo Scientific, USA) and 1:1 mixed. pRS41Hs plasmid backbone for *xylR* was prepared by PCR using primers xylR-backbone-F/-R and template pRS41Hs-xylR-WT-GFPmut2. PCR product was purified using GeneJET PCR Purification Kit (Thermo Scientific, USA). Purified PCR product was digested by *Dpn* I restriction enzyme, gel extraction was performed to remove plasmid template completely. About 0.2 pmol plasmid backbone and 0.6 pmol DNA fragments of *xylR*

https://dx.doi.org/10.1021/acssynbio.0c00225
ACS Synth. Biol. 2020, 9, 2714−2722

mutants were mixed and assembled in 40 μL Gibson assembly reaction at 50 °C for 1 h. Gibson assembly product was purified using PCR Purification Kit and eluted in 20 μL deionized water (DI H_2O), and subsequently mixed with 200 μL NEB10β-ΔxylR-ΔxylAB competent cells. The DNA-cell mixture was split into four electroporation cuvettes and electroporated as described above. Transformants were plated with 10^5, 10^6, and 10^7 dilutions on LB agar. The rest of the cells were incubated in 4 mL LB with 50 μg/mL ampicillin and 10 g/L xylose at 30 °C for 5 h.

Library size was determined by the number of transformants with 10^5, 10^6, and 10^7 dilutions on the plates. The expected number of distinct sequences obtained by ep-PCR is 9×10^6 which was calculated using an online calculator PEDEL[31] with library size 1×10^7. After 5-h incubation of the transformants, cells were diluted and subjected to FACS using BD FACSAria Fusion cell sorter (BD Bioscience, USA). By comparing fluorescence of the transformants with mutation library to the negative cells with pRS41Hs empty plasmid, all the positive cells were collected. The collected cells were spun down and resuspended in 3 mL LB. After overnight incubation, cell culture was transferred 1:50 to 3 mL fresh LB with 1 g/L xylose. After 5-h incubation, cells were subjected to FACS, and the 15% of the cells with lowest fluorescence were collected. The collected cells were incubated overnight in 3 mL LB and transferred 1:50 to 3 mL fresh LB with 5 g/L xylose. After 5-h incubation, cells were subjected to FACS and 15% of the cells with medium fluorescence were collected and plated on LB agar with 10 g/L xylose. The rest of the cells were incubated in LB for preparing glycerol stock. Described above is a three-step FACS for screening mutant *xylR*.

Mutant Identification and Fluorescence Measurement. A total of 92 single colonies and four control colonies with *xylR-WT* were picked from plates and grown in 500 μL LB in 96-deep-well plates (Thermo Scientific, USA) which were shaken at 1000 rpm in a Multitron Pro incubator (Infors HT, Switzerland) at 30 °C. After overnight incubation, cell culture was transferred 1:50 to 500 μL LB with 0, 1, 2.5, and 5 g/L xylose and incubated for 5 h. Subsequently, fluorescence of cells was measured using flow cytometer (BD Accuri C6, BD Bioscience, USA). The excitation and emission wavelength of green fluorescence were 488 nm and 530 ± 30 nm, respectively. Acquired data was analyzed using FlowJo software (BD Bioscience, USA). Geometric average of fluorescence was exhibited in this study.

The cells exhibited increased fluorescence with the increase of xylose concentration (0, 1, 2.5, and 5 g/L) were selected for further investigation. Then, mutants *xylRmut17* and *xylRmut36* with promising performance were identified. To ensure that the evolved performance was due to *xylR* mutation, coding sequences of *xylRmut17* and *xylRmut36* were amplified and reinserted in pRS41Hs-GFPmut2 plasmid backbone. Fluorescence response of strains carrying reconstructed plasmids pRS41Hs-xylRmut17-GFPmut2 and pRS41Hs-xylRmut36-GFPmut2 were investigated in the presence of different xylose levels. Specifically, cells were inoculated from 20% glycerol stocks stored at −80 °C into 3 mL LB. Cultures were grown at 30 °C overnight with 225 rpm orbital shaking and transferred 1:50 (initial $OD_{600} \sim 0.06$) into 500 μL LB with 0, 1, 2, 3, 4, 5, 6, 7, 8, 9, and 10 g/L xylose. Cell density was measured by Ultraspec 2100 pro (GE Healthcare Bio-Sciences AB, USA) at 600 nm (OD_{600}).

Plasmids carrying mutants *xylRmut17+36*, *xylRmut36a*, and *xylRmut36b* were constructed by Gibson assembly of PCR-linearized plasmid with plasmid pRS41Hs-xylRmut36-GFPmut2 as template, using primers xylRmut17-F/-R, xylRmut36a-F/-R, and xylRmut36b-F/-R, respectively. The resulting plasmids pRS41Hs-xylRmut17+36-GFPmut2, pRS41Hs-xylRmut36a-GFPmut2, and pRS41Hs-xylRmut36b-GFPmut2 were transformed into strain NEB10β-ΔxylR-ΔxylAB, resulting strains NEB10β-ΔxylR-ΔxylAB-xylRmut17+36-GFPmut2, NEB10β-ΔxylR-ΔxylAB-xylRmut36a-GFPmut2, and NEB10β-ΔxylR-ΔxylAB-xylRmut36b-GFPmut2.

BioLector Assay. To measure the dynamic response of fluorescence of whole population to different xylose levels, *E. coli* cells contain various *xylR* mutants were inoculated into 3 mL LB from −80 °C stored glycerol stock. After overnight incubation, cultures were inoculated in 1 mL LB with 0, 0.5, 1, 2, 3, 4, and 6 g/L (48 well MTP, FlowerPlate, m2p-labs, Germany). The initial OD_{600} was 0.06, cultures were incubated at 30 °C with 1000 rpm shaking using BioLector Pro (m2p-labs, Germany). Fluorescence and biomass of each well were measured every 1 h until 24 h.

Quantitative PCR Analysis. To measure transcription levels of GFPmut2 in the presence of different xylose levels, quantitative PCR (qPCR) analysis was performed. *E. coli* cultures were grown in triplicate with a starting $OD_{600} \sim 0.01$ in 2 mL LB with 0, 0.5, 1, 1.5, and 2 g/L xylose in 48-deep-well plate (Thermo Scientific, USA). The plate was incubated at 30 °C with 300 rpm orbital shaking for 15 h. One hundred microliter culture was added into 100 μL PBS (Phosphate-Buffered Saline, Thermo Scientific, USA) in 96-well plate. Fluorescence and biomass of each well were measured by microplate reader (Tecan Infinite 200 pro, Tecan, Switzerland). One milliliter of cell culture was centrifuged and cell pellet was washed with DI H_2O for RNA extraction (Quick-RNA Miniprep Kit, Zymo Research, USA). Extracted RNA was reverse transcribed using ProtoScript II First Strand cDNA Synthesis Kit (New England Biolabs, USA). qPCR analysis was performed by normalizing the RNA concentration to 20 ng/μL in each reaction (Power SYBR Green PCR Master Mix, Thermo Scientific, USA) and quantification in triplicate (ViiA 7 Real-Time PCR System, Life Technologies, USA). Transcription levels of GFPmut2 were measured relative to that of the housekeeping gene *hcaT*.[32] Primers used for quantification were listed in Table S3.

β-Galactosidase Assay and Lycopene Measurement. Mutant *xylRmut17* was amplified using primers xylR-F/-R and template pRS41Hs-xylRmut17-GFPmut2. Wild-type *xylR* in pRS41Hs-xylR-WT-lacZ and pRS41Hs-xylR-WT-crtEBI was replaced by *xylRmut17*, resulting plasmids pRS41Hs-xylRmut17-lacZ and pRS41Hs-xylRmut17-crtEBI. The plasmids were transformed into NEB10β-ΔxylR-ΔxylAB, resulting strains NEB10β-ΔxylR-ΔxylAB-xylRmut17-lacZ and NEB10β-ΔxylR-ΔxylAB-xylRmut17-crtEBI. For β-galactosidase assay, strains NEB10β-ΔxylR-ΔxylAB-xylR-WT-lacZ, NEB10β-ΔxylR-ΔxylAB-xylRmut17-lacZ were inoculated in 3 mL LB from −80 °C stored glycerol stock and cultivated overnight. Overnight cultures were transferred into 2 mL LB with 0, 0.5, 1, 2, 3, and 4 g/L xylose and, 0, 0.2, 0.4, 0.5, 0.6, 0.8, and 1.0 g/L xylose (two 48-deep-well plates) with initial $OD_{600} \sim 0.01$. For lycopene detection, plasmids pRS41Hs-xylR-WT-crtEBI and pRS41Hs-xylRmut17-crtEBI were additionally transformed into strain NEB10β-ΔxylR, resulting

https://dx.doi.org/10.1021/acssynbio.0c00225
ACS Synth. Biol. 2020, 9, 2714−2722

strains NEB10β-ΔxylR-xylR-WT-crtEBI and NEB10β-ΔxylR-xylRmut17-crtEBI. Strains NEB10β-ΔxylR-xylR-WT-crtEBI, NEB10β-ΔxylR-xylRmut17-crtEBI, NEB10β-ΔxylR-ΔxylAB-xylR-WT-crtEBI, and NEB10β-ΔxylR-ΔxylAB-xylRmut17-crtEBI were inoculated in 3 mL LB from −80 °C stored glycerol stock and cultivated overnight. Overnight cultures were transferred into 2 mL LB with 0, 0.2, 0.4, 0.5, 0.6, 0.8, and 1.0 g/L xylose (48-deep-well plate) with initial OD_{600} ∼ 0.01. After 15-h cultivation at 30 °C and 300 rpm, 1 mL cell cultures were obtained, and cell pellets were collected for measuring β-galactosidase activity[33] or lycopene production[34] using the previously reported methods.

■ ASSOCIATED CONTENT

Supporting Information

The Supporting Information is available free of charge at https://pubs.acs.org/doi/10.1021/acssynbio.0c00225.

Tables S1−S3, strains, plasmids, and primers used in this study; Figure S1, xylose utilization of the *E. coli* strains; Figure S2, map of the biosensor plasmid; Figure S3, sigmoidal dose response of biosensors; Figure S4, response of red fluorescence protein mKate2; Figure S5, fluorescence distribution of cells; Figure S6, fluorescence of cells with $XylR^{L73P,N220T}$ and $XylR^{N220T,S370A}$ under blue light; Figure S7, response of GFPmut2 to arabinose; Figure S8, transcriptional response to fluorescence response of GFPmut2; Figure S9, cell growth of strains with lycopene synthetic pathway genes (PDF)

■ AUTHOR INFORMATION

Corresponding Authors

Hal S. Alper − *McKetta Department of Chemical Engineering, The University of Texas at Austin, Austin, Texas 78712, United States;* orcid.org/0000-0002-8246-8605; Phone: +1-512-471-4417; Email: halper@che.utexas.edu

Xin-Qing Zhao − *State Key Laboratory of Microbial Metabolism, Joint International Research Laboratory of Metabolic & Developmental Sciences, School of Life Sciences and Biotechnology, Shanghai Jiao Tong University, Shanghai 200240, China;* orcid.org/0000-0002-0190-6571; Phone: +86-21-3420-6673; Email: xqzhao@sjtu.edu.cn

Authors

Rui-Qi Tang − *State Key Laboratory of Microbial Metabolism, Joint International Research Laboratory of Metabolic & Developmental Sciences, School of Life Sciences and Biotechnology, Shanghai Jiao Tong University, Shanghai 200240, China*

James M. Wagner − *McKetta Department of Chemical Engineering, The University of Texas at Austin, Austin, Texas 78712, United States*

Feng-Wu Bai − *State Key Laboratory of Microbial Metabolism, Joint International Research Laboratory of Metabolic & Developmental Sciences, School of Life Sciences and Biotechnology, Shanghai Jiao Tong University, Shanghai 200240, China*

Complete contact information is available at: https://pubs.acs.org/10.1021/acssynbio.0c00225

Author Contributions

RQT designed and performed the experiments, analyzed the data, and wrote the draft of the manuscript. JMW designed and constructed the initial xylose biosensor plasmid and edited the manuscript. HSA, XQZ, and FWB supervised the project and edited the manuscript. All authors read and agreed with the final version of the manuscript.

Notes

The authors declare no competing financial interest.

■ ACKNOWLEDGMENTS

The authors appreciate financial support from National Science Foundation of China (No. 21536006) and the Air Force Office of Scientific Research under Award No. FA9550-14-1-0089. This project is also supported by the Open Project of the State Key Laboratory of Microbial Metabolism in China (MMLKF19-01). The authors are grateful to Shuo-Fu Yuan in the University of Texas at Austin for providing the plasmids and assistance in experiments. Rui-Qi Tang was supported by China Scholarship Council.

■ REFERENCES

(1) Zhang, F., Carothers, J. M., and Keasling, J. D. (2012) Design of a dynamic sensor-regulator system for production of chemicals and fuels derived from fatty acids. *Nat. Biotechnol. 30*, 354−359.

(2) Shen, X., Wang, J., Li, C., Yuan, Q., and Yan, Y. (2019) Dynamic gene expression engineering as a tool in pathway engineering. *Curr. Opin. Biotechnol. 59*, 122−129.

(3) Lin, J. L., Wagner, J. M., and Alper, H. S. (2017) Enabling tools for high-throughput detection of metabolites: metabolic engineering and directed evolution applications. *Biotechnol. Adv. 35*, 950−970.

(4) Leavitt, J. M., Wagner, J. M., Tu, C. C., Tong, A., Liu, Y., and Alper, H. S. (2017) Biosensor-enabled directed evolution to improve muconic acid production in *Saccharomyces cerevisiae*. *Biotechnol. J. 12*, 1600687.

(5) Choi, K. R., Jang, W. D., Yang, D., Cho, J. S., Park, D., and Lee, S. Y. (2019) Systems metabolic engineering strategies: integrating systems and synthetic biology with metabolic engineering. *Trends Biotechnol. 37*, 817−837.

(6) Balzer, S., Kucharova, V., Megerle, J., Lale, R., Brautaset, T., and Valla, S. (2013) A comparative analysis of the properties of regulated promoter systems commonly used for recombinant gene expression in *Escherichia coli*. *Microb. Cell Fact. 12*, 26.

(7) Bloom, J. D., and Arnold, F. H. (2009) In the light of directed evolution: pathways of adaptive protein evolution. *Proc. Natl. Acad. Sci. U. S. A. 106* (Suppl 1), 9995−10000.

(8) Trudeau, D. L., and Tawfik, D. S. (2019) Protein engineers turned evolutionists-the quest for the optimal starting point. *Curr. Opin. Biotechnol. 60*, 46−52.

(9) Flachbart, L. K., Sokolowsky, S., and Marienhagen, J. (2019) Displaced by deceivers: prevention of biosensor cross-talk is pivotal for successful biosensor-based high-throughput screening campaigns. *ACS Synth. Biol. 8*, 1847−1857.

(10) Ni, L., Tonthat, N. K., Chinnam, N., and Schumacher, M. A. (2013) Structures of the *Escherichia coli* transcription activator and regulator of diauxie, XylR: an AraC DNA-binding family member with a LacI/GalR ligand-binding domain. *Nucleic Acids Res. 41*, 1998−2008.

(11) Ribeiro, L. F., Bressan, F., Furtado, G. P., Meireles, F., and Ward, R. J. (2013) D-xylose detection in *Escherichia coli* by a xylose binding protein-dependent response. *J. Biotechnol. 168*, 440−445.

(12) Łukasiak, J., Olsen, K., Georgiou, C. A., and Georgakopoulos, D. G. (2014) Bacterial reporter strains for D-xylose content analysis in arabinoxylans. *Eur. Food Res. Technol. 238*, 275−283.

(13) Wei, W. P., Shang, Y., Zhang, P., Liu, Y., You, D., Yin, B. C., and Ye, B. C. (2020) Engineering prokaryotic transcriptional activator

XylR as a xylose-inducible biosensor for transcription activation in yeast. *ACS Synth. Biol. 9*, 1022−1029.
(14) Song, S., and Park, C. (1997) Organization and regulation of the D-xylose operons in *Escherichia coli* K-12 XylR acts as a transcriptional activator. *J. Bacteriol. 179*, 7025−7032.
(15) Jagtap, S. S., and Rao, C. V. (2018) Microbial conversion of xylose into useful bioproducts. *Appl. Microbiol. Biotechnol. 102*, 22.
(16) Kwak, S., Jo, J. H., Yun, E. J., Jin, Y. S., and Seo, J. H. (2019) Production of biofuels and chemicals from xylose using native and engineered yeast strains. *Biotechnol. Adv. 37*, 271−283.
(17) Liu, C. G., Xiao, Y., Xia, X. X., Zhao, X. Q., Peng, L., Srinophakun, P., and Bai, F. W. (2019) Cellulosic ethanol production: progress, challenges and strategies for solutions. *Biotechnol. Adv. 37*, 491−504.
(18) Teo, W. S., and Chang, M. W. (2015) Bacterial XylRs and synthetic promoters function as genetically encoded xylose biosensors in *Saccharomyces cerevisiae*. *Biotechnol. J. 10*, 315−322.
(19) Wang, M., Li, S., and Zhao, H. (2016) Design and engineering of intracellular-metabolite-sensing/regulation gene circuits in *Saccharomyces cerevisiae*. *Biotechnol. Bioeng. 113*, 206−215.
(20) Hector, R. E., Mertens, J. A., and Nichols, N. N. (2019) Development and characterization of vectors for tunable expression of both xylose-regulated and constitutive gene expression in *Saccharomyces* yeasts. *New Biotechnol. 53*, 16−23.
(21) Szeliova, D., Krahulec, J., Safranek, M., Liskova, V., and Turna, J. (2016) Modulation of heterologous expression from P_{BAD} promoter in *Escherichia coli* production strains. *J. Biotechnol. 236*, 1−9.
(22) Cheng, F., Tang, X. L., and Kardashliev, T. (2018) Transcription factor-based biosensors in high-throughput screening: advances and applications. *Biotechnol. J. 13*, e1700648.
(23) Cormack, B. P., Valdivia, R. H., and Falkow, S. (1996) FACS-optimized mutants of the green fluorescent protein (GFP). *Gene 173*, 33−38.
(24) Yuan, S. F., and Alper, H. S. (2019) Metabolic engineering of microbial cell factories for production of nutraceuticals. *Microb. Cell Fact. 18*, 46.
(25) Alper, H., Miyaoku, K., and Stephanopoulos, G. (2005) Construction of lycopene-overproducing *E. coli* strains by combining systematic and combinatorial gene knockout targets. *Nat. Biotechnol. 23*, 5.
(26) Mcnerney, M. P., and Styczynski, M. P. (2017) Precise control of lycopene production to enable a fast-responding, minimal-equipment biosensor. *Metab. Eng. 43*, 46−53.
(27) Yoon, S. H., Lee, Y. M., Kim, J. E., Lee, S. H., Lee, J. H., Kim, J. Y., Jung, K. H., Shin, Y. C., Keasling, J. D., and Kim, S. W. (2006) Enhanced lycopene production in *Escherichia coli* engineered to synthesize isopentenyl diphosphate and dimethylallyl diphosphate from mevalonate. *Biotechnol. Bioeng. 94*, 1025−1032.
(28) Tan, S. Z., and Prather, K. L. (2017) Dynamic pathway regulation: recent advances and methods of construction. *Curr. Opin. Chem. Biol. 41*, 28−35.
(29) Datsenko, K. A., and Wanner, B. L. (2000) One-step inactivation of chromosomal genes in *Escherichia coli* K-12 using PCR products. *Proc. Natl. Acad. Sci. U. S. A. 97*, 6640−6645.
(30) Gibson, D. G., Young, L., Chuang, R. Y., Venter, J. C., Hutchison, C. A., 3rd, and Smith, H. O. (2009) Enzymatic assembly of DNA molecules up to several hundred kilobases. *Nat. Methods 6*, 343−345.
(31) Patrick, W. M., Firth, A. E., and Blackburn, J. M. (2003) User-friendly algorithms for estimating completeness and diversity in randomized protein-encoding libraries. *Protein Eng., Des. Sel. 16*, 451−457.
(32) Zhou, K., Zhou, L., Lim, Q., Zou, R., Stephanopoulos, G., and Too, H. P. (2011) Novel reference genes for quantifying transcriptional responses of *Escherichia coli* to protein overexpression by quantitative PCR. *BMC Mol. Biol. 12*, 18.
(33) Zhang, X., and Bremer, H. (1995) Control of the *Escherichia Coli rrnB* P1 promoter strength by ppGpp. *J. Biol. Chem. 270*, 9.
(34) Yoon, S. H., Kim, J. E., Lee, S. H., Park, H. M., Choi, M. S., Kim, J. Y., Lee, S. H., Shin, Y. C., Keasling, J. D., and Kim, S. W. (2007) Engineering the lycopene synthetic pathway in *E. coli* by comparison of the carotenoid genes of *Pantoea agglomerans* and *Pantoea ananatis*. *Appl. Microbiol. Biotechnol. 74*, 131−139.

https://dx.doi.org/10.1021/acssynbio.0c00225
ACS Synth. Biol. 2020, 9, 2714−2722